Structural, electronic and thermodynamic properties of half-metallic Co$_2$CrZ(Z=Ga, Ge and As) alloys: First-principles calculations

N. Bouzouira [a], D. Bensaid [a], M. Ameri [a,d,*], Y. Azzaz [a,d], N. Moulay [a,d], A. Zenati [a,d], I. Ameri [d], D. Hachemane [a], Dinesh Varshney [b], U. Hashim [c], Y. Al-Douri [c]

[a] Laboratory Physico-Chemistry of Advanced Materials, University of Djillali Liabes, BP 89, Sidi-Bel-Abbes 22000, Algeria
[b] Materials Science Laboratory, School of Physics, Vigyan Bhavan, Devi Ahilya University,Khandwa Road Campus, Indore 452001, India
[c] Institute of Nano Electronic Engineering, University Malaysia Perlis, 01000 Kangar,Perlis, Malaysia
[d] Physics Department, University of Sidi-Bel-Abbes, 22000 Sidi-Bel-Abbes, Algeria

ARTICLE INFO

ABSTRACT

Using first principles calculations, the structural, electronic, and magnetic properties of ferromagnetic half-metallic full-Heusler Co$_2$CrZ ($Z =$ Ga, Ge and As) alloy via the FP-LAPW method in the generalized gradient (GGA) and GGA+U approximations are compared with other experimental and theoretical results. The calculated equilibrium lattice constants were in qualitative agreement with the previous results. The existence of the energy gap in the minority spin (DOS and band structure) of Co$_2$CrZ ($Z =$ Ga, Ge and As) are an indication of being a potential half-metallic ferromagnetic HMF. The half-metallicity of the obtained material may prove useful for applications in spin-polarizers and spin-injectors of magnetic nanodevices. The calculated total spin magnetic moments are almost exactly that expected from Slater–Pauling rule. Thermal effects on some macroscopic properties of Co$_2$CrZ ($Z =$ Ga, Ge and As) are predicted using the quasi-harmonic Debye model, in which the lattice vibrations are taken into account. The variations of the primitive cell volume, volume expansion coefficient, bulk modulus, heat capacity and Debye temperature with pressure and temperature in the ranges of 0–20 GPa and 0–3000 K, respectively are obtained successfully.

© 2015 Elsevier Ltd. All rights reserved.

1. Introduction

Heusler alloys (HA) have attracted a significant attention due to their interesting physical properties promising various practical applications in the fields of smart materials and magneto-electronics [1]. Indeed, certain Co$_2$Y-where Y is transition elements (Ni, Co, Fe, Mn, Cr, Ti, V, etc.) -based

full-Heusler alloys (FHA) is predicted to be ferromagnetic and half-metallic i.e., compounds for which only one spin channel presents a gap at the Fermi level, while the other has a metallic character, leading to 100% carrier spin polarization at the Fermi energy (E_F) [2]. Half-metallicity has attracted much attention because of its prospective applications in spintronics [3]. Therefore, fabrication and investigation of the electronic structure and physical properties of Co$_2$Y -based FHA are of fundamental and technological interests.

The important aspect of the half-metallic Heusler alloys is their unique magneto-optical (MO) properties: a discovery of giant Kerr rotation in half-Heusler PtMnSb alloy opens the way for applications in MO reading-recording. [4] Optical

* Corresponding author at: Laboratory Physico-Chemistry of Advanced Materials, University of Djillali Liabes, BP 89, Sidi-Bel-Abbes 22000, Algeria. Tel.: +213 7 72 53 44 47.
E-mail addresses: lttnsameri@yahoo.fr, mohammed.ameri@univ-sba.dz (M. Ameri).
URL: http://univ-sba.dz/lpcma/ (M. Ameri).

and MO properties of a number of half-metallic FHA's have been investigated theoretically and experimentally. [5] Rai and Thapa [6] have investigated the electronic structure and magnetic properties of Co₂Mn Z (Z=Ge, Sn)-type Heusler compounds using first principles calculations [6].

In the present work, we investigate and discuss the bulk electronic structure, magnetic and thermodynamic properties of $Co_2CrZ(Z = Ga, Ge$ and As) alloys using the density functional first-principles calculations on the basis of the full-potential linear muffin-tin orbital (FP-LMTO) and the generalized gradient approximation (GGA) for the exchange correlation term.

The manuscript is organized as follows: in Section 2, we give details of the computational methodology and structural models. Section 3 contains the results and discussion and Section 4 summarizes the conclusion.

2. Method of calculations

The calculations reported here were carried out using *ab initio* full-potential linear muffin-tin orbital (FP-LMTO) method [7–10] as implemented in the Lmtart code [11]. The exchange and correlation potential was calculated using the generalized gradient approximation (GGA) [12] and GGA+U, By means of the option of the effective Coulomb-exchange interaction ($U_{eff} = U − J$) was used here for the calculations, the values $U_{eff} = 1.59$ eV and 1.92 eVfor Cr(3d) and Co(3d), respectively. The FP-LMTO is an improved method compared to previous LMTO techniques, and treats muffin-tin spheres and interstitial regions on the same footing, leading to improvements in the precision of the eigenvalues. At the same time, the FP-LMTO method, in which the space is divided into an interstitial regions (IR) and non-overlapping muffin-tin spheres (MTS) surrounding the atomic sites, uses a more complete basis than its predecessors. In the IR regions, the basis set consists of plane waves. Inside the MT spheres, the basis sets is described by radial solutions of the one particle Schrödinger equation (at fixed energy) and their energy derivatives multiplied by spherical harmonics. The charge density and the potential are represented inside the MTS by spherical harmonics up to $l_{max}=6$. The integrals over the Brillouin zone are performed up to 35 special **k**-points for binary compounds and 27 special **k**-points for the alloys in the irreducible Brillouin zone (IBZ) using Blochl's modified tetrahedron method [13]. The self-consistent calculations are considered to be converged when the total energy of the system is stable within 10^{-6} Ry. In order to avoid the overlap of atomic spheres, the MTS radius for each atomic position is taken to be different for each composition. We point out that the use of the full-potential calculation ensures that the calculation is not completely independent of the choice of sphere radii. Structural properties of Co₂CrGe alloy are calculated using Murnaghan's equation of state [14]

$$E(V) = E_0 + \frac{B_0 V}{B'_0}\left(\frac{(V_0/V)^{B'_0}}{B'_0 - 1} + 1\right) - \frac{B_0 V_0}{B'_0 - 1} \quad (1)$$

where E_0 is the total energy of the supercell, V_0 is the unit volume, B_0 is the bulk modulus at zero pressure and B'_0 is the derivative of bulk modulus with pressure.

3. Results and discussion

3.1. The crystal structure

Experimentally, Heusler alloys crystallizes at ambient conditions in the cubic L2₁ structure (space group Fm-3-m) with chemical formula X₂YZ (X=Co, Y=Cr and Z=Ga, Ge and As). The X atoms are placed on 8*a* X (1/4,1/4,1/4), 4*a* Y (1/2,1/2,1/2) and 4*b* Z (0,0,0) positions.

The calculated total energies within GGA as a function of the volume were used for determination of theoretical lattice constant and bulk modulus. Equilibrium lattice constant, isothermal bulk modulus, and its pressure derivative are calculated by fitting the calculated total energy to Murnaghan's equation of state [14].

The plot of energy versus volume is shown in Fig. 1. The volume corresponds to the lowest energy is used to determine equilibrium lattice constant. We summarize the calculated structural parameters and bulk modulus Co₂CrZ (Z = Ga, Ge and As) systems in Table 1 using the GGA and GGA+U approaches.

It is clear from the table that our calculated results using GGA+U Co₂CrGe(As) alloy are in good agreement with the available calculated data. To the best of our knowledge, there are no comparable studies in literature. We have compared the calculated results of Co₂CrGe(As) with its homologous systems like Co₂MnGe, Co₂CrGa and Co₂FeGe. The experimental lattice parameters of Co₂MnGe and Co₂CrGa are 5.743 Å [21] and 5.805 Å [15], respectively. Uvarov et al. have calculated the lattice constants of Co₂FeGe alloy using GGA and GGA+U which are 5.75 Å [22]. The bulk modulus given by GGA+U for Co₂CrAs is in reasonable agreement with other theoretical calculations [20]. While, the bulk modulus given by GGA+U is smaller than that corresponding GGA for the three compounds.

3.2. Magnetic moment and half- metallicity

The calculated total moment of Co₂CrZ (Z = Ga, Ge and As) within the muffin-tin spheres of the relevant Co, Cr, and Z(Ga, Ge and As) atoms for the Heusler compounds are shown in Table 2, which agrees with the Slater–Pauling curve quite well. In half-metallic Heusler alloys, the Fermi level locates in the minority energy gap, so their magnetic moments are integral values and can be described by the S–P curve of $N−24$, where N is total number of the valence electrons and 24 means that there are 12 occupied spin-down states per unit cell as has already been reported in Ref. [25]. For 3d transition metals and their binary compounds, the total spin magnetic moment (m_s^{tot}) shows the well-known Slater–Pauling behavior [26]. Thus the $Co_2CrZ(Z = Ga, Ge$ and As) alloys are with 28, 29 and 30 valence electrons, respectively. For example, the N for Co₂CrGa is $2Co(3d^7 4s^2)+Cr(3d^4 4s^2)+Ga(4s^2 4p^1) = 27$, it has the total magnetic moment of 3 μ_B. The replacement of Ga by Ge and As leads to increase the total magnetic moment (Cr magnetic moment down) to 2.993, 3.936 and 4.90 μ_B(1.427, 2.002 and 2.578 μ_B) using GGA in Co₂CrZ(Z = Ga, Ge and As) alloys. The Co magnetic moment increases along Ga–Ge–As series

a

b

c

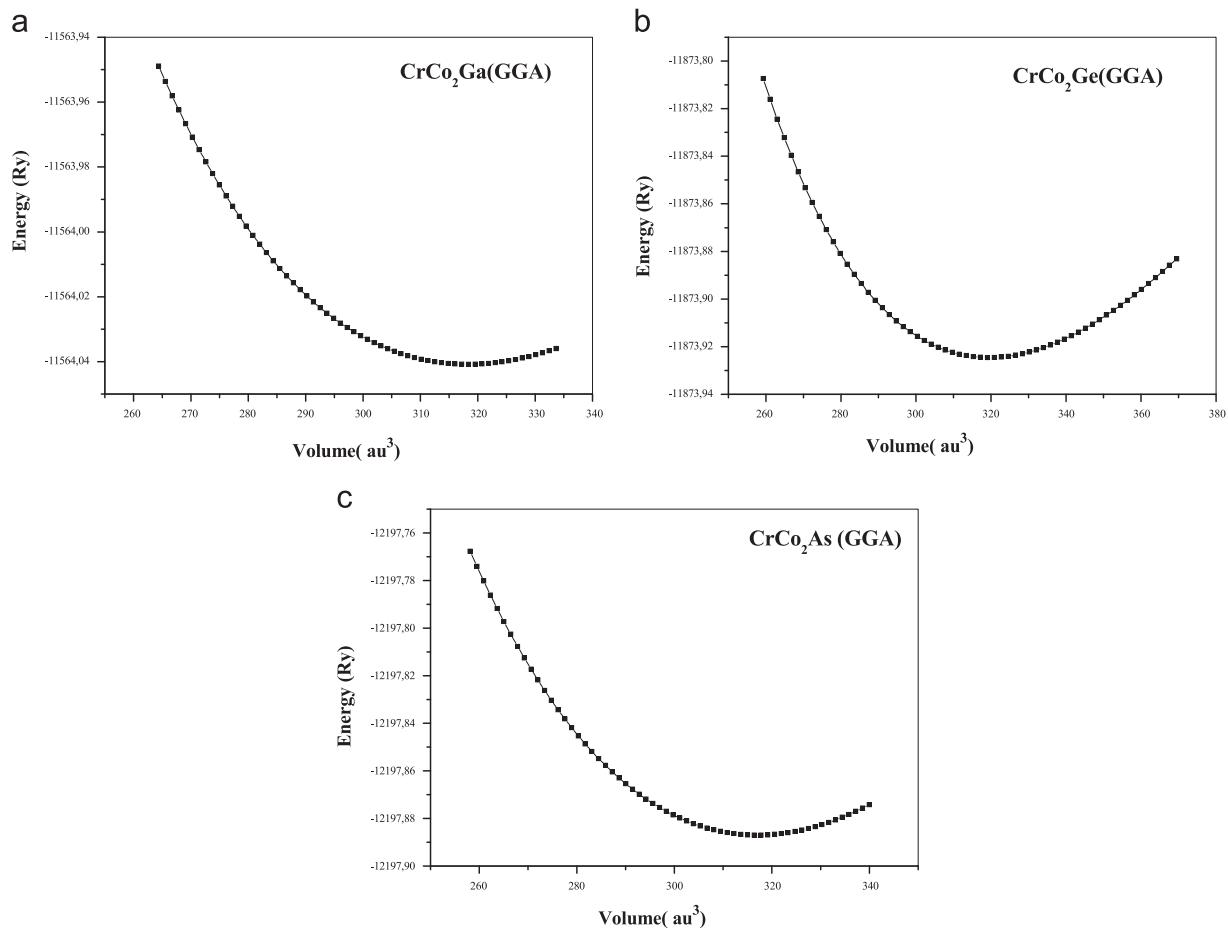**Fig. 1.** Calculated total energy for three compounds $Co_2CrZ(Z = Ga, \ Ge \ and \ As)$ as functions of volume cell.

due to decreasing of Co–Cr hybridization for minority spin states.

The local spin magnetic moments on the non-transition metal atoms Ga(Ge and As) is small and aligned antiparallel to that of the Co and Cr atoms. The calculated m_s^{tot} for GGA+U approach is almost exactly that expected from Slate Paulin $m_s^{tot}Co_2CrZ(Z = Ga, \ Ge \ and \ As) = 3.156$, 4.004 μ_B and , 5.01 μ_B, respectively. While, the calculated m_s^{tot} using GGA approximately is different. Thus, Rai et al. [17] have reported the total magnetic moment of the alloys $m_s^{tot}(Co_2CrZ)(Z = Ga, \ Ge \ and \ As) = 3.03, \ 3.999 \ and 4.891$ μ_B , respectively [17]. Tung et al. [24] have calculated for Co_2CrGe the total magnetic moment of $m_s^{tot}(Co_2CrGe)$ $= 3.997 \ \mu_B$.

These values for the magnetic moments of the Co_2CrZ $(Z = Ga, \ Ge \ and \ As)$ have obtained using GGA (GGA+U) are in good agreement with the previous results shown in Table 2.

3.3. Spin polarization and half-metallic

The spin polarization of a magnetic material is defined by

$$P_N = \frac{N\uparrow - N\downarrow}{N\uparrow + N\downarrow} \tag{2}$$

where $N\uparrow$ and $N\downarrow$ are the number of↑spin and↓spin states at E_F, respectively. Under this definition, P_N measures the spin imbalance of mobile electrons. It has also been defined, alternatively, as the net fractional spin polarization near E_F. In this case, we denote it by P to distinguish from P_N, with

$$P = \frac{d\uparrow - d\downarrow}{d\uparrow + d\downarrow} \tag{3}$$

where $d\uparrow$ and $d\downarrow$ are the density of states (DOS) of↑spin and↓spin channels at E_F, respectively. P can therefore be directly determined from the DOS.

The spin polarization P would then vary from -1.0 to 1.0 only. For the half-metallic materials, P equals to either -1.0 or 1.0. The calculated $\uparrow(E_F)$, $d\downarrow(E_F)$ and P for the Heusler compounds are shown in Table 3. In the present work, we studied the Co_2CrGe alloy which shows 100% spin polarization at E_F (Table 3). According to our result, the compound Co_2CrGe is interesting as it shows large DOS at the E_F of $d\downarrow(E_F) = 1.71$ states/eV (Table 3). The reason for the big value is that E_F cuts through strongly localized states of Cr-d, whereas the contribution of Co-d states to $d\downarrow(E_F)$ is very small as shown in Fig. 2a. On the other hand, $d\uparrow(E_F) = 0$ states/eV for both Co and Cr atoms;

Table 1

Lattice constants a and bulk modulus B correspond to experimental results and other theoretical calculations of $Co_2CrZ(Z = Ga, Ge$ and As).

		Lattice constant a (Å)	Bulk modulus B (GPa)	Pressure derivative B'
Co_2CrGa present	GGA	5.735	213.26	4.21
	GGA+U	5.740	190.40	4.49
	Exp	5.805[a]		
	Previous.	5.879[b], 5.802[c]	262.69[c]	
Co_2CrGe present	LSDA	5.608	250.71	4.63
	GGA	5.742	203.94	4.53
	GGA+U	5.752	194.85	4.63
	Previous.	5.74[d], 5.77[e]	250.43[e]	7.47[e]
Co_2CrAs present	GGA	5.727	248.78	2.74
	GGA+U	5.796	176.44	4.79
	Previous.	5.785[f], 5.81[c]	179.3[f],192.39[c]	

[a] Ref [15].
[b] Ref [16].
[c] Ref [17].
[d] Ref [18].
[e] Ref [19].
[f] Ref [20].

Table 2

Total and partial magnetic moments of $Co_2CrZ(Z = Ga, Ge$ and As).

Magnetic moment (μ_B) of $Co_2CrZ(Z = Ga, Ge$ and As)

	Co	Cr	Z	total
Co_2CrGa GGA	0.804	1.427	−0.042	2.993
GGA+U	0.791	1.778	−0.057	3.156
Other calc [23]	0.758	1.651	−0.053	3.051
[17]	0.737	1.602	−0.064	3.03
Co_2CrGe GGA	0.976	2.002	−0.018	3.936
GGA+U	0.944	2.213	−0.044	4.004
Other calc[24]	0.932	2.122	−0.029	3.999
[23]	0.950	2.129	−0.033	3.997
Co_2CrAs GGA	1.13	2.598	0.048	4.90
GGA+U	1.099	2.656	0.019	5.01
Other calc[17]	1.066	2.578	0.044	4.891
[20]	1.98	2.95	0.07	5.00

according to this, Co_2CrGe is a half metal which gives -1.0 spin polarizations at E_F.

The calculated partial densities of states for Co_2CrZ(Ga, Ge and As) using GGA and GGA+U are shown in Fig. 2. It is clear from that the compounds Co_2CrZ(Ga, Ge and As) are half-metallic with the E_F falling in the spin–dn insulating gap. It is seen that the main contributions to the resulting DOS of three compounds obtained by either GGA(GGA+U) methods are due to the Co and Cr atoms. The Co-3d and Cr-3d states are hybridized between 0.75 eV and 5.3 eV in the conduction bands (Fig. 2b). The most intense peaks of the DOS are formed by the coincident in energy Co and Cr states. A detailed analysis shows that the contribution to the hybridized states is mainly due to the Co and Cr 3d states, which indicates a covalent character of their interaction. The contribution to the total DOS from the Ge states is small. This means that the Ge atoms form essentially ionic bonds with the surrounding atoms.

The calculations of the electronic band structure along the symmetry lines of Brillouin zone are shown in Fig. 3 indicate that the↓spin channel is conducting. The top of the valence band is taken as the zero of energy. In this compound, the valence band maximum (VBM) is located at point Γ whereas the conduction band minimum (CBM) is located at point X, resulting in indirect band gap of 0.36(0.44) and 0.28(0.61) eV for Co_2CrZ(Ga, Ge), respectively, via GGA(GGA+U), while the minority spin band structure of Co_2CrAs has direct band gap along Γ direction with $E_{gap}=0.52$ eV.

The band gap values for some of the compounds using GGA+U method are also shown in Table 3. It is clear that electron–electron correlation may create or destroy the gap or shift E_F outside the gap.

The (E_F) lies in the middle of the gap of the majority spin states, The formation of gap for the half-metal compounds was discussed by Galanakis et al. [25]. This value is in good agreement with the previous calculated data. However, these results are smaller than compared with the homologous systems like Co_2MnGe [27] and Co_2CrGa [16].

3.4. Thermodynamic properties

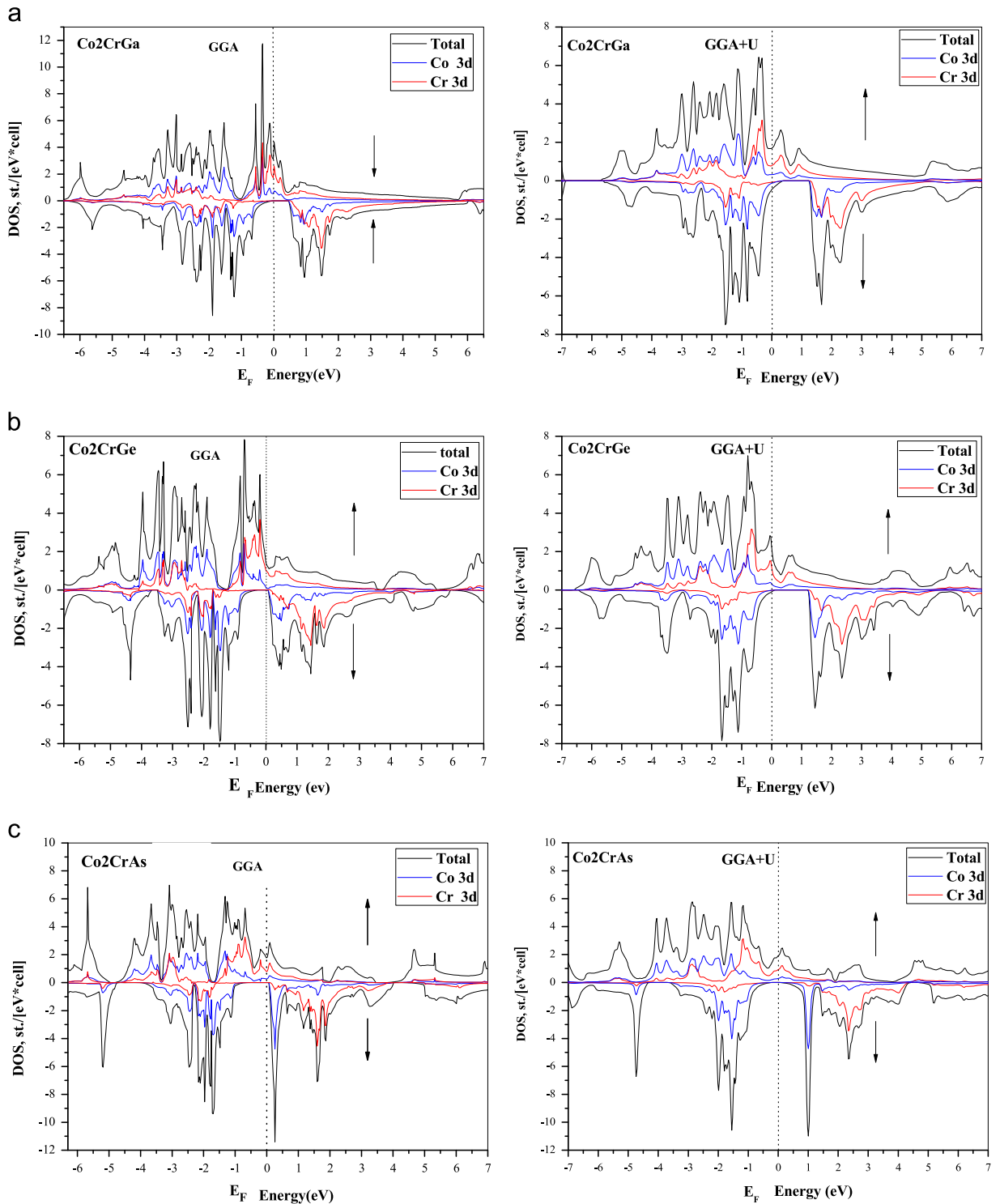In this study, the quasi-harmonic Debye model [28–31] is used to obtain the thermodynamic properties of Co_2CrGe. in

Table 3

Energy gap and spin polarization of $Co_2CrZ(Z = Ga, Ge$ and As).

		Energy band gap E_g (eV)			Spin polarization		
		$E_{max}(I)$	$E_{min}(X)$	ΔE	$d\uparrow(E_F)$	$d\downarrow(E_F)$	P%
Co_2CrGa	GGA	0.071	0.439	0.368	3.709	0.005	99.73
	GGA+U	0.154	0.595	0.441	1.693	−0.459	57.34
Other calc	[17]	0.0	0.28	0.28	4.2	0.0	100
	[24]				2.928	0.215	86.36
Co_2CrGe	GGA	−0.076	0.208	0.284	0.00	1.71	100
	GGA+U	−0.119	0.493	0.612	2.30	0.00	100
Other calc	[21]	0.0	0.24	0.24	3.00	0.00	100
	[24]				2.82	0.00	100
	[23]						99.8
Co_2CrAs	GGA	−0.633	−0.105	0.52	1.765	0.0	100
	GGA+U	−0.246	0.108	0.345	1.913	0.0	100
Other calc	[17]	−0.50	−0.10	0.4	2.8	0.6	70
	[20]			0.4			

Fig. 2. Spin-projected total and partial DOS for (a) Co_2CrGa, (b) Co_2CrGe and (c) Co_2CrAs.
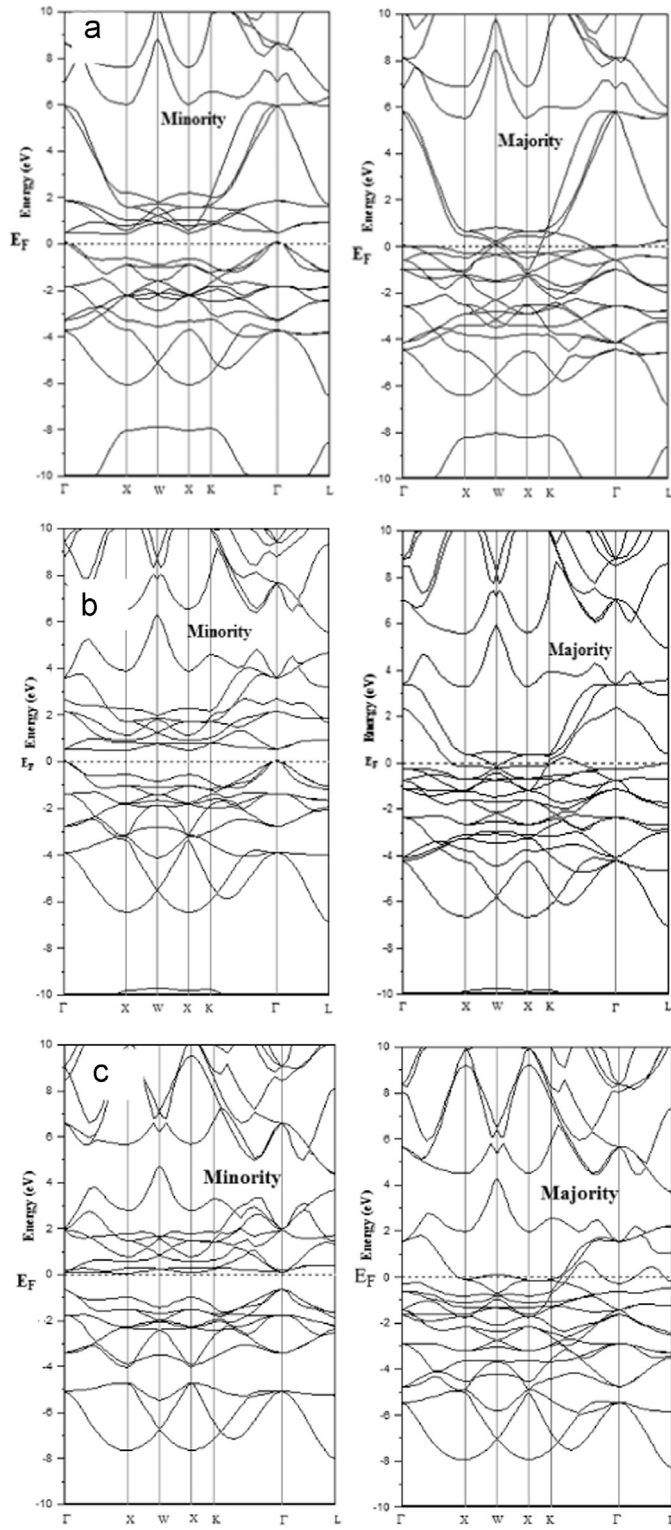
Fig. 3. Band structure for (*a*) Co$_2$CrGa, (b)Co$_2$CrGe and (*c*)Co$_2$CrAs.
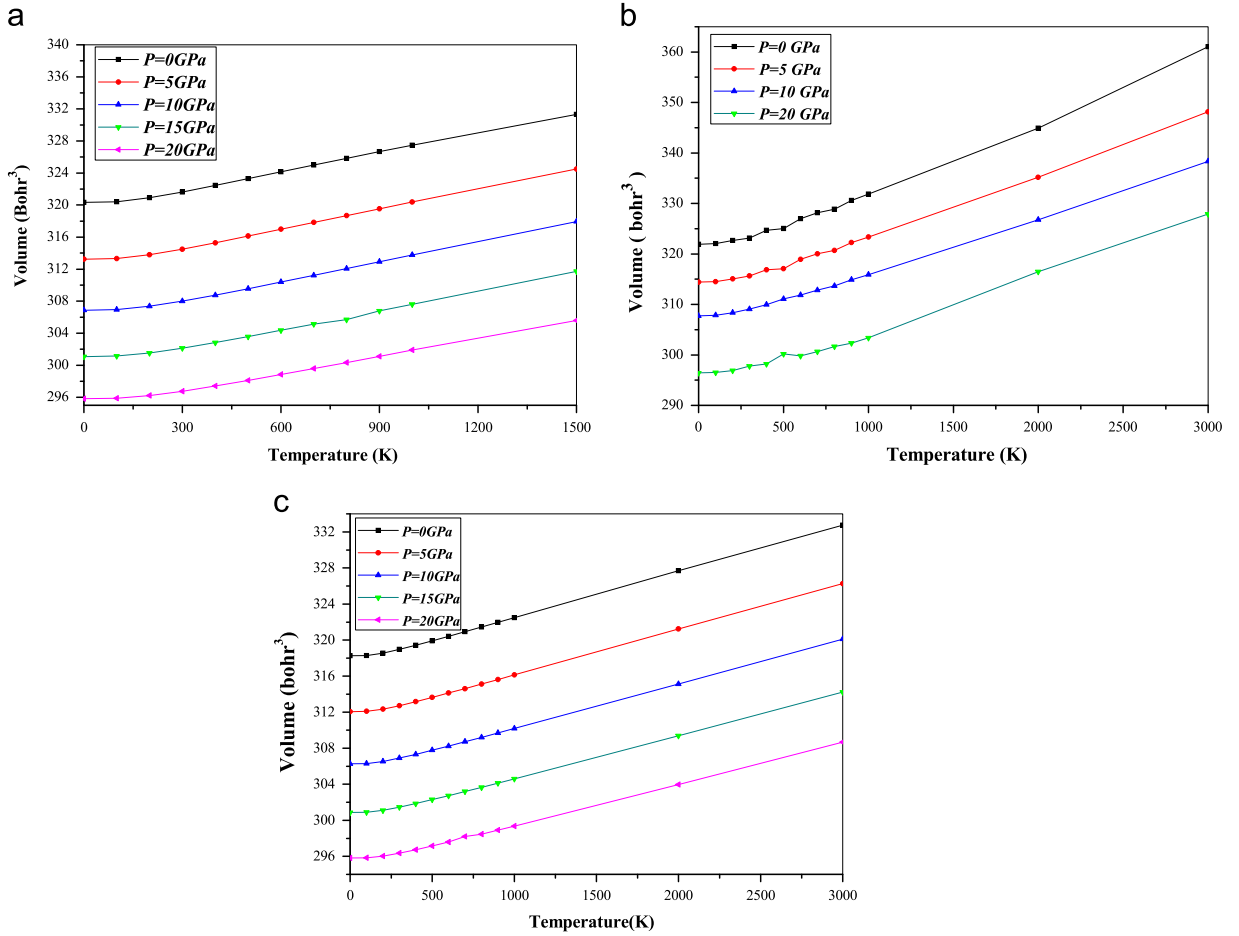
Fig. 4. Variation of the primitive cell volume with temperature at different pressures for (*a*) Co$_2$CrGa, (b)Co$_2$CrGe and (*c*)Co$_2$CrAs.

which The non-equilibrium Gibbs function $G^*(V, P, T)$ is expressed as:

$$G^*(V, P, T) = E(V) + PV + A_{vib}[\theta(V); T] \quad (4)$$

where $E(V)$ is the total energy per unit cell for Co$_2$CrGe, PV is the constant hydrostatic pressure condition, $\theta(V)$ is the Debye temperature, and the vibrational

Helmholtz free energy A_{vib} can be written as [29,30]:

$$A_{vib}(\Theta; T) = nkT\left[\frac{9}{8}\frac{\Theta}{T} + 3\ln\left(1 - e^{-\Theta/T}\right) - D\left(\frac{\Theta}{T}\right)\right] \quad (5)$$

where n is the number of atoms per formula unit, $D(\Theta/T)$ is the Debye integral. For an isotropic solid [32]

$$\Theta = \frac{\hbar}{K}\left[6\pi^2 V^{1/2} n\right]^{1/3} f(\sigma)\sqrt{\frac{B_S}{M}} \quad (6)$$

where M is the molecular mass per unit cell and B_S is the adiabatic bulk modulus. The non-equilibrium Gibbs function $G^*(V, P, T)$ as a function of $(V; P, T)$ can be minimized with respect to volume V as:

$$\left[\frac{\delta G^*(V, P, T)}{\delta V}\right]_{P,T} = 0 \quad (7)$$

The thermal properties such as internal energies, entropy, heat capacity at constant volume C_V, and thermal

expansion α are taken as:

$$U = nkT\left[\frac{9}{8}\frac{\theta}{T} + 3D\left(\frac{\Theta}{T}\right)\right] \quad (8)$$

$$S = nK\left[4D\left(\frac{\Theta}{T}\right) - 3\ln\left(1 - e^{-\frac{\Theta}{T}}\right)\right] \quad (9)$$

$$C_V = 3nk\left[4D\left(\frac{\Theta}{T}\right) - \frac{3\Theta/T}{e^{\Theta/T - 1}}\right] \quad (10)$$

$$\alpha = \frac{\gamma C_v}{B_T V} \quad (11)$$

Here γ is the Grüneissen parameters which are given by the following equation [27]:

$$\gamma = -\left(\frac{d\ln\Theta(V)}{d\ln V}\right) \quad (12)$$

The thermal properties are determined in the temperature range from 0 to 3000 K, where the quasi-harmonic model remains fully valid. The pressure effect is studied in the 0–20 GPa range.

The dependence of the primitive cell volume on the temperature using GGA is shown in Fig. 4. The volume increases almost linearly with increasing temperature. For a given temperature $T = 300$ K and zero pressure,
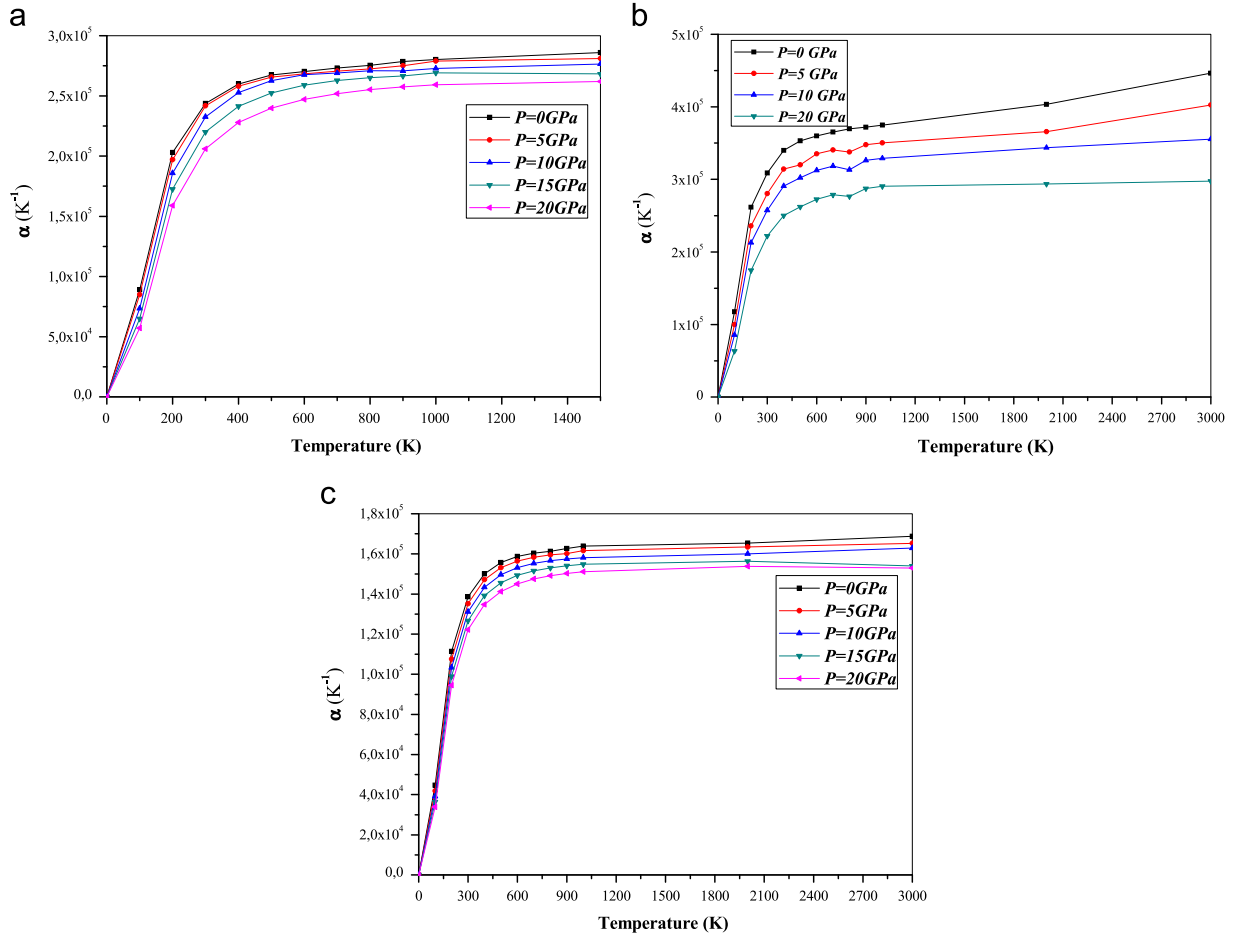
Fig. 5. Variation of the thermal expansion coefficient with temperature at different pressures for (a) Co_2CrGa, (b)Co_2CrGe and (c)Co_2CrAs.

the primitive cell volume alters with increasing pressure via GGA for $Co_2CrZ(Z = Ga, Ge$ and As) alloys to be 321.62 μa^3, 323.11 μa^3 and 318.95 μa^3, respectively.

The second-order polynomial fitting of V–P data gives the following equations at $T = 300$ K, for three alloys:

$$\{V(P) = 321.6243 - 1.4801P + 0.0118P^2 (Co_2CrGa) \quad (13)$$
$$\{V(P) = 323.1179 - 1.5513P + 0.0143P^2 (Co_2CrGe) \quad (14)$$
$$\{V(P) = 318.952 - 1.2812P + 0.0076P^2 (Co_2CrAs) \quad (15)$$

$$Co_2CrGa \begin{cases} \alpha(T) = 9.3927 \times 10^3 + 1.0518 \times 10^3 T - 1.2485T^2 + 4.478 \times 10^{-4}T^3 (P = 0 \text{ GPa}) \\ \alpha(P) = 2.4367 \times 10^5 + 5.1029 \times 10^2 P - 2.0109 \times 10^2 P^2 + 4.076P^3 (T = 300 \text{ K}) \end{cases} \quad (16, 17)$$

The variations in thermal expansion coefficient (α) with temperature and pressure are shown in Fig. 5. It is shown that, at a given pressure, α increases sharply with increasing of temperature up to 400 K. When $T > 500$ K, α gradually approaches a linear increasing with enhanced temperature and the propensity of increment becomes very moderate, which means that the temperature dependence of α is very small at high temperature. As shown in Fig. 5, for

$T > 600$ K and $P = 20$ GPa, Co_2CrGe has a fairly constant thermal expansion $\alpha = 2.87 \times 10^5$ K^{-1}. For a given temperature, α decreases drastically with increasing of pressure. Using GGA, at 300 K and zero pressure, the α values for $Co_2CrZ(Z = Ga, Ge$ and As) are 2.4367×10^5 K^{-1}, 3.089×10^5 K^{-1} and 1.385×10^5 K^{-1}, respectively.

The fit equations to third-order polynomial for α – T data at zero pressure and for α – P data at $T = 300$ K are given as:

Fig. 6 shows the variation of the bulk modulus versus temperature. The compressibility is practically constant between 0 and 300 K for $T > 600$ K then it decreases linearly with increasing temperature. For a given temperature, the bulk modulus increases with increasing pressure. The effect of increasing pressure and decreasing temperature on the bulk modulus are nearly the same. At zero pressure and $T = 300$ K, the bulk modulus for $Co_2CrZ(Z = Ga, Ge$ and As) are 214.21 GPa, 201.2 GPa and 246.63 GPa, respectively.

$$\text{Co}_2\text{CrGe} \begin{cases} \alpha(T) = 7.056 \times 10^4 + 7.412 \times 10^2 T - 0.504 T^2 + 1.045 \times 10^{-4} T^3 \ (P = 0 \text{ GPa}) \\ \alpha(P) = 3.089 \times 10^5 - 6.418 \times 10^3 P + 1.527 \times 10^2 P^2 - 2.455 P^3 \ (T = 300 \text{ K}) \end{cases} \tag{18, 19}$$

$$\text{Co}_2\text{CrAs} \begin{cases} \alpha(T) = 4.3724 \times 10^3 + 5.6809 \times 10^2 T - 0.5977 T^2 + 1.76 \times 10^{-4} T^3 \ (P = 0 \text{ GPa}) \\ \alpha(P) = 1.385 \times 10^5 - 5.962 \times 10^2 P - 17.827 P^2 + 0.3408 P^3 \ (T = 300 \text{ K}) \end{cases} \tag{20, 21}$$
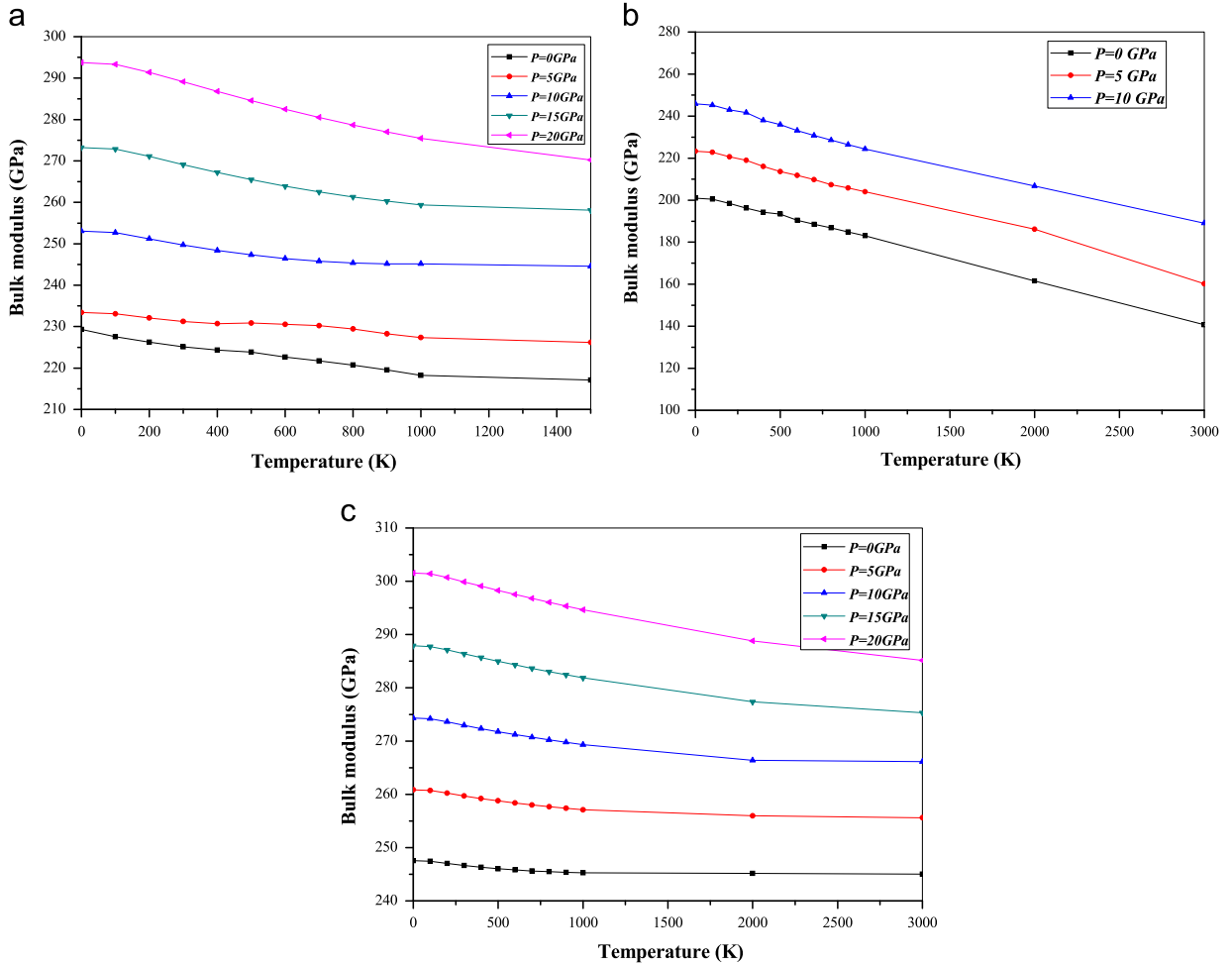

Fig. 6. Variation of the bulk modulus with temperature at different pressures for (a) Co_2CrGa, (b) Co_2CrGe and (c) Co_2CrAs.

The bulk modulus−pressure relations are obtained by fitting the *B*–*P* data at $T = 300$ K to the following third-order polynomials for $\text{Co}_2\text{CrZ}(Z = \text{Ga}, \text{Ge and As})$ alloys:

$$B(P) = 214.21 + 3.233P + 0.037P^2 - 5.933 \\ \times 10^{-4}P^3 (\text{Co}_2\text{CrGa}) \tag{22}$$

$$B(P) = 201.22 + 5.177P - 0.0487P^2 + 5.8 \\ \times 10^{-4}P^3 (\text{Co}_2\text{CrGe}) \tag{23}$$

$$B(P) = 246.63 + 2.585P - 0.005P^2 - 8.666 \\ \times 10^{-4}P^3 (\text{Co}_2\text{CrAs}) \tag{24}$$

The variation of heat capacity C_V at constant volume versus temperature at 0, 5, 10,15 and 20 GPa pressures is shown in Fig. 7. With increasing temperature, C_V values increase rapidly at a lower temperature, then increase slowly at high temperature [33,34], which is common to all alloys at high temperature. It is found that when $T < 600$ K, C_V depends on both temperature and pressure (C_V is proportional to T^3 [35]). From 0 to about 800 K, C_V increases exponentially and then at high temperature approaches approximately 99.5 J mol^{-1} K^{-1} for the three compounds. Using GGA, at zero pressure and 300 K, C_V is 48.64 mol^{-1} K^{-1}, 82.46 mol^{-1} K^{-1} and 85.49 J mol^{-1} K^{-1} for the $\text{Co}_2\text{CrZ}(Z = \text{Ga}, \text{Ge and As})$ alloys, respectively.
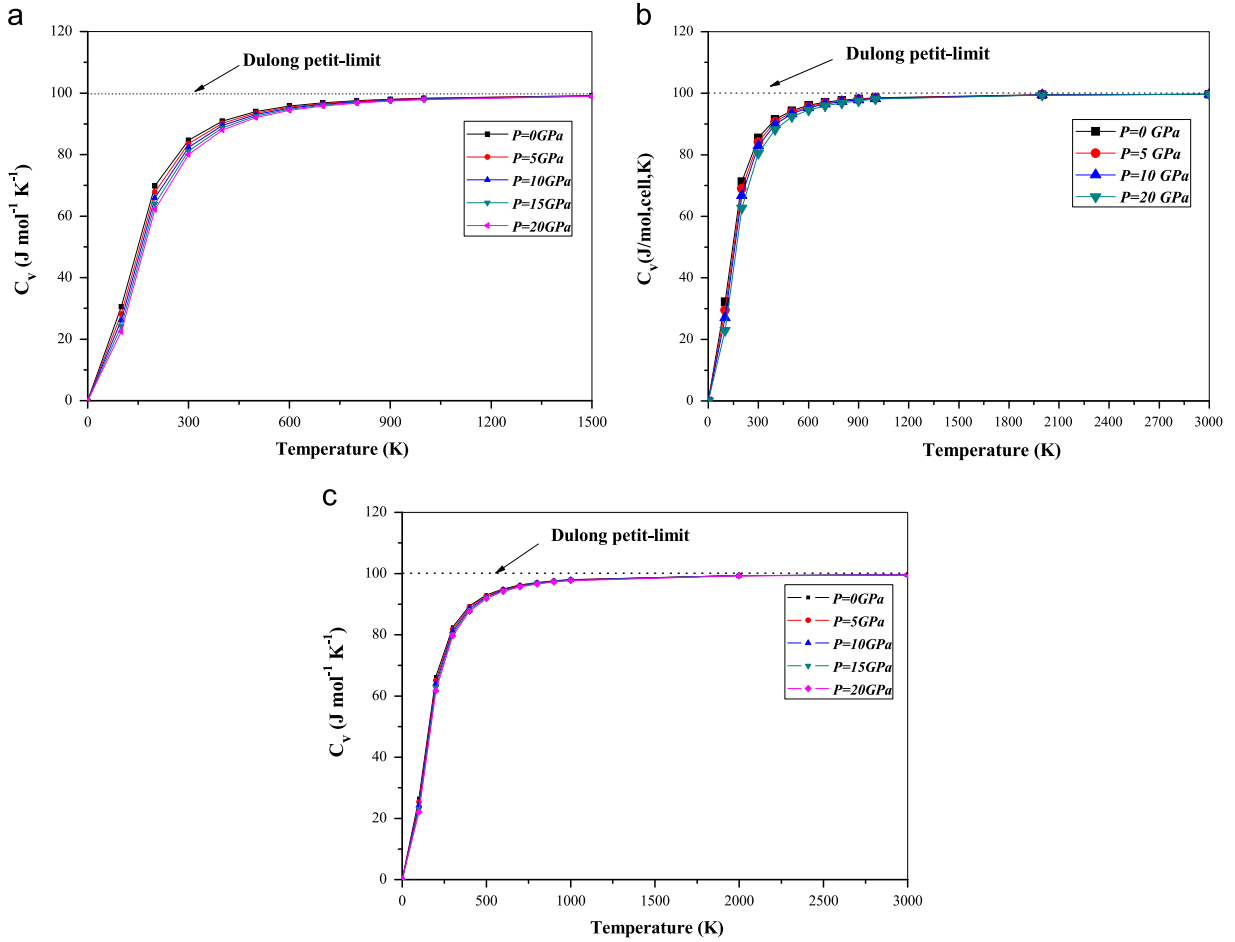
Fig. 7. Variation of the heat capacity C_v with temperature at different pressures for (*a*) Co_2CrGa, (*b*)Co_2CrGe and (*c*)Co_2CrAs.

4. Conclusion

In this work, we have investigated the electronic structure and magnetism of three half-metallic full-Heusler compounds,$Co_2CrZ(Z = Ga$, Ge and As) with a high-ordered structure using full-potential linear muffin-tin orbital (FP-LMTO) method within the generalized gradient GGA and GGA+U approximation, framework based on the density functional theory (DFT). The systems show perfect half-metallic character with semiconducting minority spin band structure, which has zero electronic density of states at Fermi level. The energy gap in minority spin channel is a direct gap at point Γ. The total magnetic moment of the $Co_2CrZ(Z = Ga,Ge$ and As) are 3,156, 4.004 and 5.01 μ_B, respectively. The results are in good agreement with the Slater–Pauling rule. We have investigated the possibility of appearance of half-metallicity in the case of the $Co_2CrZ(Z = Ga,Ge$ and As) system that shows 100% spin polarization at E_F. The existence of energy gap in minority spin (DOS and band structure) is an indication of being a potential HMF. As well as the integral value of magnetic moment is also the evident of HMF. Through the quasi-harmonic Debye model, the dependences of the lattice constant, bulk modulus, thermal expansion parameter, heat capacity and Debye temperature on temperature and pressure have been obtained successfully. It is hoped that our new results for $Co_2CrZ(Z = Ga,Ge$ and As) will be confirmed experimentally and theoretically in future.

References

[1] T. Graf, C. Felser, S.S.P. Parkin, Prog. Solid State Chem. 39 (2011) 1.
[2] W de Boeck, W van Roy, J Das, V Motsnyi, Z Liu, L Lagae, H Boeve, K Dessein, G Borghs, Semicond. Sci. Technol. 17 (2002) 342.
[3] I Zutic, J Fabian, SD Sarma, Rev. Mod. Phys. 76 (2004) 323–410.
[4] P.G. Van Engen, K.H.J. Buschow, R. Jongebreur, M. Erman, Appl. Phys. Lett. 42 (1983) 202.
[5] Y. Kubo, N. Takakura, S. Ishida, J. Phys. F: Met. Phys. 13 (1983) 161.
[6] D.P Rai, R.K. Thapa, Phase Transit.:Multinatl. J. 85 (2012) 608–618.
[7] S. Savrasov, D. Savrasov, Phys. Rev. B 46 (1992) 12181.
[8] S.Y. Savrasov, Phys. Rev. B 54 (1996) 16470.
[9] P. Hohenberg, W. Kohn, Phys. Rev. B 136 (1964) 864.

[10] W. Kohn, L.J. Sham, Phys. Rev. A 140 (1965) 1133.
[11] S.Y. Savrasov, Z. Krist. 220 (2005) 555.
[12] J.P. Perdew, Y. Wang, Phys. Rev. B 46 (1992) 12947.
[13] P. Blochl, O. Jepsen, O.K. Andersen, Phys. Rev. B 49 (1994) 16223.
[14] F.D. Murnaghan, Proc. Natl. Acad. Sci. USA 30 (1944) 244.
[15] K H J Bushow, P.G. van Engen, J. Magn. Magn. Mater. 25 (1981) 90.
[16] DP Rai, Sandeep, MP Ghimire, RK Thapa, Int. J. Mod. Phys. B 28 (2012) 1250071.
[17] D.P. Rai, et al., J. Semicond. 33 (2012) 12.
[18] M, Gilleßen,Von der Fakultat fur Mathematik Informatik und Naturwissenschaften der RWTH Aachen University zur Erlangung des akademischen Grades eines Doktors der Naturwissenschaften genehmigte Dissertation, 2009.
[19] Rai, et al., J. Theor. Appl. Phys. 7 (2013) 3.
[20] U. Kanbur, et al., J.Magn. Magn. Mater. 323 (2011) 1156–1160.
[21] P J Brown, K U Neumann, P J Webster, K R A Ziebeck, J. Phys.: Condens. Matter 12 (2000) 1827.
[22] Uvarov, et al., A Dictionary of Science Mass Market Paperback, , – 1962.
[23] Miura, Shirai, Nagao, J. Appl. Phys. 99 (2006) 08J112.
[24] Jen-Chuan Tung, Guang-Yu Guo, New J. Phys. 15 (2013) 033014.
[25] I Galanakis, P H Dederichs, Phys. Rev. B 66 (2002) 174429.
[26] C Kittel, Introduction to Solid State Physics, Wiley, New York, 1968, 470.
[27] Rai, et al., Multinatl. J. 85 (2012) 608–618.
[28] M.A. Blanco, E. Francisco, V. Lunana, Comput. Phys. Commun. 158 (2004) 57.
[29] F. Peng, H.Z. Fu, X.L. Cheng, Physica B 400 (2007) 83.
[30] F. Peng, H.Z. Fu, X.D. Yang, Solid State Commun. 145 (2008) 91.
[31] F. Peng, H.Z. Fu, X.D. Yang, Physica B 403 (2008) 2851.
[32] M.A Blanco, A.M Pend_as, E Francisco, J.M Recio, R Franko, J. Mol. Struct. (Theochem) 368 (1996) 245.
[33] M szybowicz, et al., Opto-Electr. Rev. 7 (1999) 103–106.
[34] AT Petit, PL. Dulong, Ann. Chim. Phys. 10 (1819) 395.
[35] P. Debye, Ann. Phys. 39 (1912) 789.